

AWARD NUMBER: W81XWH-12-1-0457

TITLE: Noninvasive Detection and Differentiation of Axonal Injury/Loss, Demyelination, and Inflammation

PRINCIPAL INVESTIGATOR: Sheng-Kwei Song

CONTRACTING ORGANIZATION: Washington University  
St. Louis, MO 63110-1010

REPORT DATE: October 2015

TYPE OF REPORT: Annual

PREPARED FOR: U.S. Army Medical Research and Materiel Command  
Fort Detrick, Maryland 21702-5012

DISTRIBUTION STATEMENT: Approved for Public Release;  
Distribution Unlimited

The views, opinions and/or findings contained in this report are those of the author(s) and should not be construed as an official Department of the Army position, policy or decision unless so designated by other documentation.

# REPORT DOCUMENTATION PAGE

*Form Approved  
OMB No. 0704-0188*

Public reporting burden for this collection of information is estimated to average 1 hour per response, including the time for reviewing instructions, searching existing data sources, gathering and maintaining the data needed, and completing and reviewing this collection of information. Send comments regarding this burden estimate or any other aspect of this collection of information, including suggestions for reducing this burden to Department of Defense, Washington Headquarters Services, Directorate for Information Operations and Reports (0704-0188), 1215 Jefferson Davis Highway, Suite 1204, Arlington, VA 22202-4302. Respondents should be aware that notwithstanding any other provision of law, no person shall be subject to any penalty for failing to comply with a collection of information if it does not display a currently valid OMB control number. **PLEASE DO NOT RETURN YOUR FORM TO THE ABOVE ADDRESS.**

<b>1. REPORT DATE</b> October 2015			<b>2. REPORT TYPE</b> Annual		<b>3. DATES COVERED</b> 30Sep2014 – 29Sep2015	
<b>4. TITLE AND SUBTITLE</b>  Noninvasive Detection and Differentiation of Axonal Injury/Loss, Demyelination, and Inflammation					<b>5a. CONTRACT NUMBER</b> W91ZSQ2056N615	<b>5b. GRANT NUMBER</b> W81XWH-12-1-0457
					<b>5c. PROGRAM ELEMENT NUMBER</b>	
<b>6. AUTHOR(S)</b>  Sheng-Kwei Song, William M. Spees, Peng Sun, Yong Wang, Anne Cross  E-Mail: ssong@wustl.edu					<b>5d. PROJECT NUMBER</b>	
					<b>5e. TASK NUMBER</b>	
					<b>5f. WORK UNIT NUMBER</b>	
<b>7. PERFORMING ORGANIZATION NAME(S) AND ADDRESS(ES)</b>  Washington University Campus Box 8018 660 South Euclid Ave. St. Louis, MO 63110-1010					<b>8. PERFORMING ORGANIZATION REPORT NUMBER</b>	
<b>9. SPONSORING / MONITORING AGENCY NAME(S) AND ADDRESS(ES)</b>  U.S. Army Medical Research and Materiel Command Fort Detrick, Maryland 21702-5012					<b>10. SPONSOR/MONITOR'S ACRONYM(S)</b>	
					<b>11. SPONSOR/MONITOR'S REPORT NUMBER(S)</b>	
<b>12. DISTRIBUTION / AVAILABILITY STATEMENT</b>  Approved for Public Release; Distribution Unlimited						
<b>13. SUPPLEMENTARY NOTES</b>						
<b>14. ABSTRACT</b>  During year 3 of this funding support, we have applied the developed tools to demonstrate that DBSI is the future of diffusion MRI to more accurately detect underlying white matter tract pathologies noninvasively. We have focused our effort in completing specific aim 3, the dexamethasone treatment of optic neuritis of experimental autoimmune encephalomyelitis (EAE) mice. We repeated immunohistochemical staining of all optic nerves from previous in vivo DBSI measurements to improve the quantification. Through the improved staining and the use of objective quantification approach we were able to establish the correlation of in vivo DBSI pathological metrics with corresponding Immunohistochemical staining. The most significant finding is that we have validated that DBSI derived axonal volume may be used to quantify the extent of axonal loss of optic nerve. The assessment of irreversible axonal loss in optic nerve may be extended to the rest of CNS and could potentially quantify the rate of axonal loss providing a biomarker of irreversible progression of multiple sclerosis.						
<b>15. SUBJECT TERMS</b> Multiple sclerosis, diffusion basis spectrum imaging, diffusion tensor imaging, EAE, inflammation, axonal injury, curizone, demyelination, optic neuritis, axonal loss						
<b>16. SECURITY CLASSIFICATION OF:</b>			<b>17. LIMITATION OF ABSTRACT</b> Unclassified	<b>18. NUMBER OF PAGES</b> 34	<b>19a. NAME OF RESPONSIBLE PERSON</b> USAMRMC	
<b>a. REPORT</b> Unclassified					<b>19b. TELEPHONE NUMBER (include area code)</b>	
<b>b. ABSTRACT</b> Unclassified			<b>c. THIS PAGE</b> Unclassified			

## **Table of Contents**

	<u>Page</u>
<b>1. Introduction.....</b>	<b>4</b>
<b>2. Keywords.....</b>	<b>4</b>
<b>3. Overall Project Summary.....</b>	<b>4 – 6</b>
<b>4. Key Research Accomplishments.....</b>	<b>6</b>
<b>5. Conclusion.....</b>	<b>6</b>
<b>6. Publications, Abstracts, and Presentations.....</b>	<b>6</b>
<b>7. Inventions, Patents and Licenses.....</b>	<b>6</b>
<b>8. Reportable Outcomes.....</b>	<b>6</b>
<b>9. Other Achievements.....</b>	<b>6</b>
<b>10. References.....</b>	<b>6 – 7</b>
<b>11. Appendices.....</b>	<b>8</b>

## Introduction

Acute neurological impairments in MS are associated with the combined effect of the underlying inflammation, axonal injury, and demyelination, while long-term MS disability is due to the extent of irreversible axonal damage, may or may not be dependent on the frequency or severity of relapses.<sup>1-10</sup> We employ *in vivo* diffusion basis spectrum imaging (DBSI) to simultaneously quantify axonal injury, demyelination, and inflammation in CNS white matter, correlating with postmortem immunohistochemical staining, in experimental autoimmune encephalomyelitis (EAE) mice with and without dexamethasone treatment.

## Keywords

Multiple sclerosis, diffusion basis spectrum imaging, diffusion tensor imaging, EAE, inflammation, axonal injury, demyelination, axonal loss, optic neuritis

## Overall project Summary

Our work during this funding period focused on (1) quantitatively validating *in vivo* DBSI derived axon volume obtained in specific aim 2, and (2) on imaging effect of dexamethasone treatment in optic nerve from mice of optic neuritis (specific aim 3). We summarize the progress during year 3 as the following.

### 1. Acute axonal loss in the presence of optic nerve swelling detected using *in vivo* DBSI

We continued analyzing DBSI results obtained from year 2 incorporating a new concept based on fiber fraction derived from DBSI to quantify axon volume noninvasively. We performed additional Immunohistochemical staining on paraffin-embedded tissue sections to validate this concept.

During year 2 of the current funding support, we performed longitudinal *in vivo* DBSI of 10 C57BL/6 mice before immunization. Mice were then immunized using MOG<sub>35-55</sub> peptide. At the onset of optic neuritis (ON), i.e., visual acuity (VA)  $\leq 0.25$  cycles/degree, mice were imaged and daily VA assessment continued. In this cohort of mice, unilateral ON was seen in every mouse. We therefore defined Time 1 as the day in which the first eye had a VA  $\leq 0.25$  c/d and Time 2 as the day in which the second eye had a VA  $\leq 0.25$  c/d. Concordantly, for each mouse, Eye 1 is the eye affected at Time 1 and Eye 2 is the eye affected at Time 2. Based on this

experimental paradigm, Time 1 and Time 2 corresponded to onset and post-onset of optic neuritis for Eye 1 and pre-onset and onset of optic neuritis for Eye 2, respectively. *In vivo* DBSI was performed again when the VA of the initially unaffected eye was lower than 0.25 cycles/degree. After the third DBSI examination, all mice were perfusion fixed and optic nerves excised, paraffin-embedded, sectioned, and Immunohistochemical staining performed.

In addition to previously reported correlation between *in vivo* DBSI detected optic nerve inflammation, demyelination, and axonal and the corresponding immunohistochemical staining results, we have observed optic nerve swelling during acute ON (Fig. 1). Most strikingly, DBSI detected significant axonal loss at this stage of the disease. We also quantified Immunohistochemical staining results (Fig. 2) to validate *in vivo* DBSI derived pathological metrics, including axonal injury, demyelination, increased cellularity, and axon volume (Fig. 3).

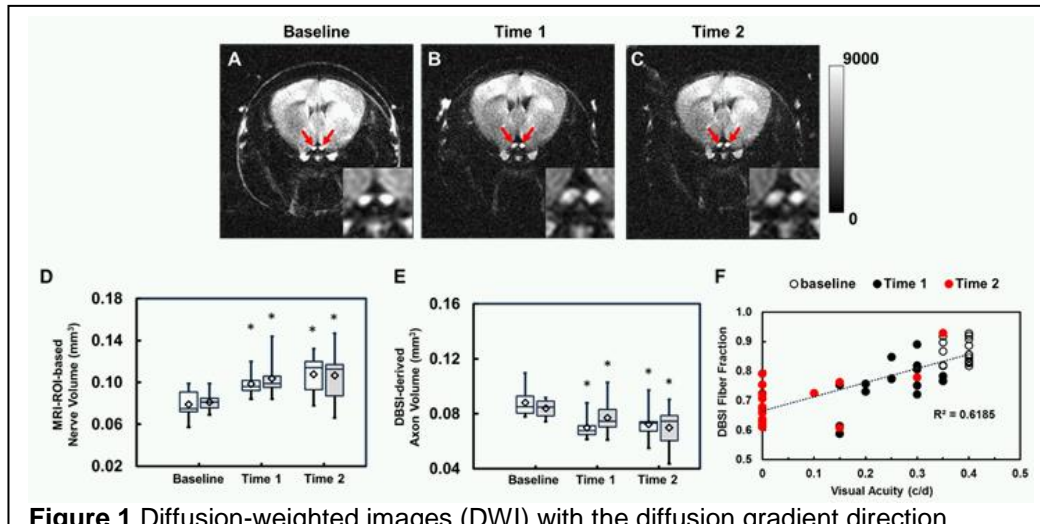


**Figure 1** Diffusion-weighted images (DWI) with the diffusion gradient direction applied perpendicular to the optic nerves (red arrows) from an representative EAE mouse at (A) baseline, i.e., before EAE, (B) Time 1, i.e., onset of ON in the first eye, and (C) Time 2, i.e., onset of ON in the second eye. Optic nerve swelling was seen at Time 1 and 2 caused by inflammation associated increase in cellularity and edema. Significantly increased optic nerve volume was seen after ON (D,  $p < 0.05$  for Eye 1 and 2). The corresponding DBSI-derived axon volume (optic nerve volume  $\times$  DBSI fiber fraction) suggested a significant axonal loss in optic nerves (E,  $p < 0.05$  for Eye 1 and 2). DBSI fiber fraction, reflecting effects of axonal loss and inflammation, correlated well with visual acuity (F). \* indicates  $p < 0.05$ .

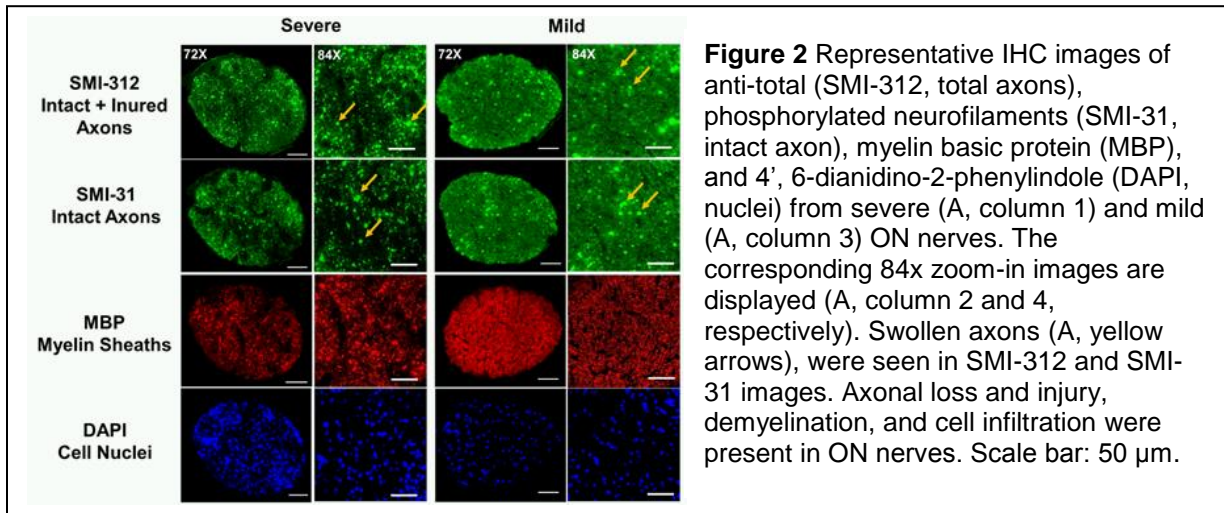
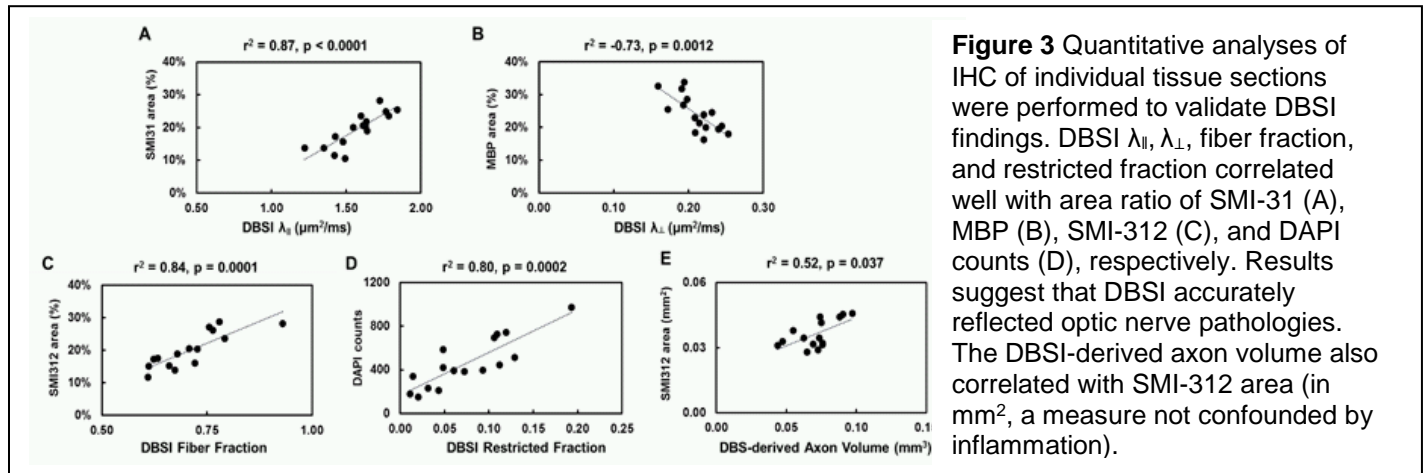


**Figure 2** Representative IHC images of anti-total (SMI-312, total axons), phosphorylated neurofilaments (SMI-31, intact axon), myelin basic protein (MBP), and 4', 6-dianidino-2-phenylindole (DAPI, nuclei) from severe (A, column 1) and mild (A, column 3) ON nerves. The corresponding 84x zoom-in images are displayed (A, column 2 and 4, respectively). Swollen axons (A, yellow arrows), were seen in SMI-312 and SMI-31 images. Axonal loss and injury, demyelination, and cell infiltration were present in ON nerves. Scale bar: 50  $\mu$ m.



## 2. In vivo DBSI to assess dexamethasone treatment

In the specific aim 3, we initially proposed to treat EAE mice beginning at the onset of ON for two weeks using dexamethasone at a dose of 0.3 mg/kg/day. After we established the protocol to longitudinally image EAE mice starting from baseline, i.e., before EAE induction, we imaged mice as planned with dexamethasone treatment. Unfortunately, 0.3 mg/kg/day of dexamethasone for two weeks failed to demonstrate a beneficial effect on the progression of ON comparing with PBS treated mice, i.e., no improvement in visual acuity with dexamethasone treatment. We increased dexamethasone dose to 3 mg/kg/day for two weeks. At the new dose, an improvement of DBSI derived pathological metrics was observed (Fig. 4). We requested and was granted a no-cost-extension to complete this new dose (3 mg/kg/day, two weeks) for treating EAE mice.

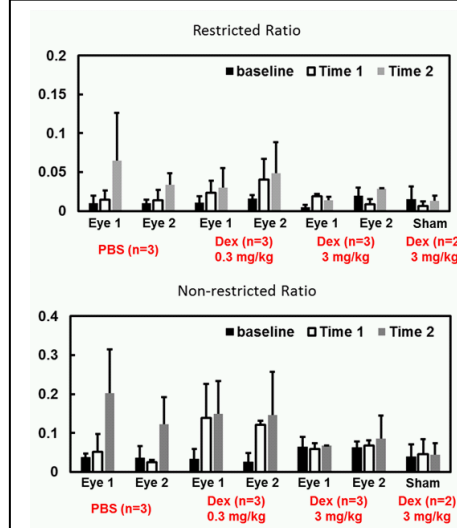


**Figure 3** Quantitative analyses of IHC of individual tissue sections were performed to validate DBSI findings. DBSI  $\lambda_{\parallel}$ ,  $\lambda_{\perp}$ , fiber fraction, and restricted fraction correlated well with area ratio of SMI-31 (A), MBP (B), SMI-312 (C), and DAPI counts (D), respectively. Results suggest that DBSI accurately reflected optic nerve pathologies. The DBSI-derived axon volume also correlated with SMI-312 area (in  $\text{mm}^2$ , a measure not confounded by inflammation).

**Changes/Problems** Currently, the two-week long 3 mg/kg/day dexamethasone treatment was on hold since 0.3 mg/kg/day (not 3 mg/kg/day) was approved in the initial animal protocol supporting this study. We have

filed a self-reported adverse event to our IACUC followed by an updated animal protocol amendment awaiting approval. A self-reported adverse event has also been submitted to ACURO pending review.

### **Key Research Accomplishments**

1. We have demonstrated that DBSI derived fiber fraction correlated with total neurofilament staining area, i.e., the axonal density, a measure of combined effect of axonal loss, and dilution effect from inflammation associated cell infiltration and edema.
2. To more accurately quantify the extent axonal loss without confounding effects of inflammation, we further developed a novel marker DBSI-“axon volume” by taking optic nerve volume into account deriving an equivalent of “axon count” to assess irreversible axonal damage. This was demonstrated in Fig. 3E where SMI-312 area in mm<sup>2</sup>, no confounding effect from inflammation, correlated well with “axon volume” derived by DBSI.
3. Based on current findings derived from EAE mice, we developed a research plan to image optic neuropathy in patients and was recently funded by National Eye Institute to translate DBSI for imaging optic nerves in patients with optic neuritis and glaucoma.

### **Conclusion**

We have overcome many obstacles to implement the proposed studies successfully demonstrating that DBSI is indeed a novel approach to image underlying reversible (inflammation, demyelination and axonal injury) and irreversible (axonal loss) pathologies in optic nerves from EAE mice at the onset of ON.

We successfully imaged optic nerves with dexamethasone treatment as proposed in specific aim 3. The proposed dose 0.3 mg/kg/day failed to suppress optic nerve inflammation. We were able to demonstrate that 3 mg/kg/day of dexamethasone treatment successfully suppressed optic nerve inflammation. In preparing this report, we realized that 3 mg/kg dexamethasone was not in the animal protocol approved by WU IACUC or ACURO. We reported this adverse event immediately and halted the study. In the meantime, an amendment of animal protocol was submitted to IACUC and was approved on January 4, 2016.

Based on results from this project, we are confident that DBSI is ready for human translation. We are currently implementing a reduced-Field-of-View diffusion MRI sequence on our human scanners to image optic nerves from patients of multiple sclerosis and glaucoma. We will test the hypothesis that the rate of irreversible axonal injury, assessed by “axon volume” derived by DBSI, can serve as a predictor of disease progression and efficacy of therapeutic interventions.

### **Publications**

1. Lin, T-N, Chiang, C-W, Perez-Torres, CJ, Sun, P, Wallendorf, M, Schmidt, RE, Wang, Y, Cross, AH, and Song, S-K, “Axonal loss occurs early in optic neuritis as quantified by diffusion basis spectrum imaging”, To be submitted to *BRAIN*.

### **Inventions, Patents and Licenses**

None

### **Reportable Outcomes**

None

### **Other Achievements**

None

### **References**

- 1 Andersen, O. Predicting a window of therapeutic opportunity in multiple sclerosis. *Brain* **133**, 1863-1865, doi:awq182 [pii] 10.1093/brain/awq182 (2010).

- 2 Bjartmar, C., Kidd, G., Mork, S., Rudick, R. & Trapp, B. D. Neurological disability correlates with spinal cord axonal loss and reduced N-acetyl aspartate in chronic multiple sclerosis patients. *Ann Neurol* **48**, 893-901 (2000).
- 3 Confavreux, C. & Vukusic, S. Natural history of multiple sclerosis: a unifying concept. *Brain* **129**, 606-616, doi:awl007 [pii] 10.1093/brain/awl007 (2006).
- 4 Constantinescu, C. S. & Gran, B. Multiple sclerosis: autoimmune associations in multiple sclerosis. *Nat Rev Neurol* **6**, 591-592, doi:nrneurol.2010.147 [pii] 10.1038/nrneurol.2010.147 (2010).
- 5 Conway, D. S. & Cohen, J. A. Multiple sclerosis: Mechanisms of disability accumulation in multiple sclerosis. *Nat Rev Neurol* **6**, 654-655, doi:nrneurol.2010.175 [pii] 10.1038/nrneurol.2010.175 (2010).
- 6 Fisniku, L. K. et al. Disability and T2 MRI lesions: a 20-year follow-up of patients with relapse onset of multiple sclerosis. *Brain* **131**, 808-817, doi:awm329 [pii] 10.1093/brain/awm329 (2008).
- 7 Frischer, J. M. et al. The relation between inflammation and neurodegeneration in multiple sclerosis brains. *Brain* **132**, 1175-1189, doi:awp070 [pii] 10.1093/brain/awp070 (2009).
- 8 Kutzelnigg, A. et al. Cortical demyelination and diffuse white matter injury in multiple sclerosis. *Brain* **128**, 2705-2712, doi:awh641 [pii] 10.1093/brain/awh641 (2005).
- 9 Scalfari, A. et al. The natural history of multiple sclerosis: a geographically based study 10: relapses and long-term disability. *Brain* **133**, 1914-1929, doi:awq118 [pii] 10.1093/brain/awq118 (2010).
- 10 Trapp, B. D. & Nave, K.-A. Multiple Sclerosis: An Immune or Neurodegenerative Disorder? *Annual Review of Neuroscience* **31**, 247-269, doi:doi:10.1146/annurev.neuro.30.051606.094313 (2008).

**Title:** Axonal loss occurs early in optic neuritis as quantified by diffusion basis spectrum imaging

**Authors:** Tsen-Hsuan Lin, PhD<sup>1,a</sup>, Chia-Wen Chiang, PhD<sup>1,a,b</sup>, Carlos J Perez-Torres, PhD<sup>1,c</sup>, Peng Sun, PhD<sup>1</sup>, Michael Wallendorf, PhD<sup>3</sup>, Robert E. Schmidt, MD, PhD<sup>4</sup>, Yong Wang, PhD<sup>1,2</sup>, Anne H Cross, MD<sup>2,5</sup>, and Sheng-Kwei Song, PhD<sup>1,2</sup>

<sup>1</sup>*Department of Radiology*, <sup>2</sup>*Hope Center for Neurological Disorders*, <sup>3</sup>*Divison of Biostatistics*,

<sup>4</sup>*Department of Pathology*, <sup>5</sup>*Department of Neurology, Washington University, Saint Louis, MO, United States*

<sup>a</sup> *These authors contributed equally to this work*

<sup>b</sup> *Current Institution: Institute of Biomedical Engineering and Nanomedicine, National Health Research Institute, Miaoli, Taiwan*

<sup>c</sup> *Current Institution: Radiological Health Sciences, School of Health Sciences, Purdue University, West Lafayette, IN, United States*

**\*Corresponding Author:**

Sheng-Kwei “Victor” Song, Ph.D.  
Biomedical MR Laboratory  
Campus Box 8227  
Washington University School of Medicine  
Room 2313, 4525 Scott Ave, St Louis, MO 63110, USA  
Fax: +1 314 362 0526  
Phone: +1 314 362 9988  
E-mail: [ssong@wustl.edu](mailto:ssong@wustl.edu)

**Number of Characters in the Title:** 792

**Words in Abstract:** 317 **Words in content:** 3054

**Number of Figures: 6 Color Figures: 2**

## **Abstract**

Magnetic resonance imaging markers have been widely used to detect and quantify central nervous system white matter pathologies in multiple sclerosis. However, the coexistence of confounding multiple pathologies prevents these image markers from accurately assessing axon and myelin pathologies. We have recently developed a diffusion basis spectrum imaging to distinguish and quantify co-existing axonal injury, demyelination, and inflammation in the central nervous system tissue of multiple sclerosis patients and animal models. In this study, we quantified optic nerve pathologies in experimental autoimmune encephalomyelitis mice at baseline (naïve, before immunization), before, during, and after the onset of optic neuritis using diffusion basis spectrum imaging. Our results demonstrated that diffusion basis spectrum imaging not only individually quantified the severity of axonal injury, demyelination, and inflammation at different time points of acute optic neuritis but also, for the first time, noninvasively detected ~18% axonal loss at the onset of optic neuritis in experimental autoimmune encephalomyelitis mice. All diffusion basis spectrum imaging detected optic nerve pathologies, including axonal injury, demyelination, increased cellularity, and axonal loss, were quantitatively validated with corresponding immunohistochemical markers. Our findings support the notion that axonal loss, a primary cause of permanent neurological impairments, could occur early in multiple sclerosis. Currently, the axonal loss of visual system is most commonly assessed by measuring the retinal nerve fiber layer thickness using optical coherence tomography. In contrast to optical coherence tomography, diffusion basis spectrum imaging detected pathologies in the posterior visual pathway unreachable by optical coherence tomography. It detected axonal loss without being confounded by optic nerve swelling resulting from the co-existing inflammation associated increase in cellularity and edema. With the

capability to detect and distinguish various nerve pathologies, diffusion basis spectrum imaging could decipher the interrelationship among various pathological components and the role each plays in disease progression. Quantification of the rate of axonal loss may fulfill the long-sought biomarker to predict treatment outcome and to determine when progressive disease starts.

## **Introduction**

Multiple sclerosis (MS) is an inflammatory demyelinating disease producing, ultimately, irreversible axonal loss and permanent neurological impairments [1-4]. The axonal pathology is complex with components directly associated with the fiber tracts (axonal injury/loss and demyelination) and those surrounding the tracts (immune cell infiltration and edema). Each of these axonal pathology components contributes to neurological dysfunction and therefore to the clinical signs and symptoms of MS [4-6]. Although inflammation and demyelination each contributes to MS pathophysiology, axonal loss is believed to be the primary correlate of irreversible neurological disability [7, 8]. Therefore, the development of a non-invasive biomarker to reflect the extent of axonal loss and the severity of damage in residual axons is paramount to better care for individual patients with MS, and to use as an endpoint in trials of potential therapeutics. Optic neuritis is commonly one of the first manifestations of MS [9, 10]. Optic neuritis, much like MS, is characterized by inflammatory demyelination and axonal injury [10]. Optic nerve dysfunction leads to impairment of visual function which can be monitored in mice in a clinically relevant manner [11]. As such, mouse models of optic neuritis present an opportunity to evaluate the connection between imaging, pathology and function in MS.

Several different magnetic resonance imaging (MRI) MRI biomarkers have recently been evaluated in MS [12-14]. Diffusion tensor imaging (DTI), in particular, is one of the commonest tools for evaluating white matter disease as it can distinguish axonal injury from demyelination [15-17]. However DTI-derived metrics are obfuscated by the presence of inflammatory pathology [18, 19]. We recently developed a new diffusion MRI approach called diffusion basis spectrum imaging (DBSI) that is able to separately quantify the axonal and inflammatory pathologies [20,

21]. DBSI models the diffusion signal as a linear combination of anisotropic diffusion tensors reflecting fibers, which in white matter are predominantly axon fibers, and a spectrum of isotropic diffusion tensors which encompass cells, edema and cerebrospinal fluid [20, 22]. In the study reported here, we applied DBSI at the onset of optic neuritis (ON) in the experimental autoimmune encephalomyelitis (EAE) mouse model. DBSI is able to distinguish and quantify axon injury, demyelination, cellular infiltration and edema, and axonal loss. Our results demonstrated that DBSI could be a means to reflect axonal pathology longitudinally and could potentially serve as an outcome measure for assessing efficacy of treatments.

## **Materials and Methods**

### *EAE Mouse Model of Optic Neuritis*

All experiments were approved by the Washington University Animal Studies Committee and were performed on 8-week old female C57BL/6 mice (The Jackson Laboratory, Bar Harbor, ME). The EAE model of optic neuritis was induced as previously described [22]. Mice were immunized with 50 µg myelin oligodendrocyte peptide (MOG<sub>35-55</sub>) emulsified in incomplete Freund's adjuvant with 50 µg *Mycobacterium tuberculosis*. Mice further received 300 ng intravenous adjuvant pertussis toxin (PTX, List Laboratories, Campbell, CA) on the day of and two days after immunization. Eight mice were studied.

### *Visual Acuity (VA) Measurements*

VA was utilized to measure visual function in parallel to clinical signs. VA was measured with the Virtual Optometry System (Optometry, Cerebral Mechanics, Inc., Canada) as previously described [23]. In short, mice were presented with virtual rotating columns displayed on 4 LCD screens. The spatial frequencies in cycle/degree (c/d) was changed starting from 0.1 c/d with step size of 0.05

c/d until the mouse stopped responding. VA is then defined as the highest spatial frequency to which the mouse was able to respond. If the mouse did not respond to 0.1 c/d, VA was assigned to be 0 c/d. With this technique it is possible to separately assess the VA of each eye by switching the rotational direction of the columns. Visual impairment was defined as  $VA \leq 0.25$  c/d, based on our previous work [22]. Normal VA was confirmed before immunization and then assessed daily after immunization.

For each mouse in our cohort, onset of optic neuritis, as indicated by impairment of visual function defined by VA, did not occur simultaneously for both eyes. We therefore defined Time 1 as the day in which the first eye had a  $VA \leq 0.25$  c/d and Time 2 as the day in which the second eye had a  $VA \leq 0.25$  c/d. Concordantly, for each mouse, Eye 1 is the eye affected at Time 1 and Eye 2 is the eye affected at Time 2. VA for each eye is presented in (Fig 1). Based on this experimental paradigm, Time 1 and Time 2 corresponded to onset and post-onset of optic neuritis for Eye 1 and pre-onset and onset of optic neuritis for Eye 2, respectively.

#### *Magnetic Resonance Imaging (MRI) Measurements*

MRI experiments were performed on a 4.7 T Agilent DirectDrive™ small-animal MRI system (Agilent Technologies, Santa Clara, CA) equipped with Magnex/Agilent HD imaging gradient coil (Magnex/Agilent, Oxford, UK) with pulse gradient strength up to 58 G/cm and a gradient rise time  $\leq 295$   $\mu$ s. Mice were anesthetized with 1% isoflurane in oxygen and placed in a custom made 3-point immobilization head holder. Breathing rate was monitored and body temperature was maintained at 37° C with a small animal physiological monitoring and control unit (SA Instruments, Stony Brook, NY). An actively-decoupled volume (transmit)/surface (receive) coil

pair was used for MRI excitation and signal reception. Diffusion weighted MRI data was acquired with a transverse slice of mouse brain with two optic nerves, as nearly orthogonal to the image slice as possible. A multi-echo spin-echo diffusion-weighted sequence [24] with an icosahedral 25-direction diffusion-encoding scheme [25] combined with one  $b=0$  was employed and MR acquisition parameters were TR of 1.5 s, TE of 37 ms, time between gradient pulses ( $\Delta$ ) of 18 ms, gradient pulse duration ( $\delta$ ) of 6 ms, maximum  $b$ -value of 2200 s/mm<sup>2</sup> (each encoding direction has a unique  $b$ -value), slice thickness of 0.8 mm, and in-plane resolution of 117  $\mu\text{m}$  by 117  $\mu\text{m}$ .

### *MRI Data Analysis*

Data was analyzed with DBSI multi-tensor and conventional DTI single-tensor analysis packages developed in-house with Matlab [20, 21]. For DBSI, the imaging data was modeled according to Equation 1:

$$S_k = \sum_{i=1}^{N_{Aniso}} f_i e^{-|\vec{b}_k| \lambda_{\perp i}} e^{-|\vec{b}_k| (\lambda_{\parallel i} - \lambda_{\perp i}) \cos^2 \psi_{ik}} + \int_a^b f(D) e^{-|\vec{b}_k| D} dD \quad (k = 1, 2, 3, \dots, 25). \quad [1]$$

The quantities  $S_k$  and  $|\vec{b}_k|$  are the signal and  $b$ -value of the  $k^{\text{th}}$  diffusion gradient,  $N_{Aniso}$  is the number of anisotropic tensors (fiber tracts),  $\Psi_{ik}$  is the angle between the  $k^{\text{th}}$  diffusion gradient and the principal direction of the  $i^{\text{th}}$  anisotropic tensor,  $\lambda_{\parallel i}$  and  $\lambda_{\perp i}$  are the axial and radial diffusivities of the  $i^{\text{th}}$  anisotropic tensor,  $f_i$  is the signal intensity fraction for the  $i^{\text{th}}$  anisotropic tensor, and  $a$  and  $b$  are the low and high diffusivity limits for the isotropic diffusion spectrum (reflecting cellularity and edema, respectively)  $f(D)$ . For optic nerve, we have a coherent fiber bundle. DBSI derived  $f_i$  represents retinal ganglion cell (RGC) axon density (fiber fraction) in the image voxel, accounting for intra-voxel pathological and structural complications. Based on prior work, DBSI derived  $\lambda_{\parallel}$  and  $\lambda_{\perp}$  reflect residual axon and myelin integrity respectively:  $\downarrow \lambda_{\parallel} = \text{axonal}$

injury and  $\uparrow \lambda_{\perp}$  = demyelination [12-14]. Based on our previous experimental findings, the restricted isotropic diffusion fraction reflecting cellularity is derived by the summation of  $f(D)$  at  $0 \leq \text{ADC} \leq 0.3 \text{ } \mu\text{m}^2/\text{ms}$ . The summation of the remaining  $f(D)$  at  $3 > \text{ADC} > 0.3 \text{ } \mu\text{m}^2/\text{ms}$  represents non-restricted isotropic diffusion, which denotes vasogenic edema and CSF [20, 22, 26].

Regions of interest (ROI) were manually drawn in the center of each optic nerve on the diffusion-weighted image, which corresponded to the diffusion gradient direction perpendicular to optic nerves, to minimize partial volume effects. ROIs were then transferred to the parametric maps to calculate the mean for each of the DBSI and DTI-derived metrics.

#### *ROI for DBSI fiber fraction*

Separate ROIs encompassing the whole optic nerve were drawn on the orthogonal-optic-nerve DWI, which were larger than the ROIs for measuring DBSI- or DTI-derived metrics. The ROIs for DBSI fiber fraction were not affected by the partial volume effect of surrounding cerebrospinal fluid. The fiber signal was modeled separating from isotropic components during DBSI analyses.

#### *Immunohistochemistry (IHC)*

Immediately after the final MRI time point, mice underwent perfusion via the left cardiac ventricle with PBS followed by 4% paraformaldehyde (PFA). Brains were excised and fixed for another 24 hours in 4% PFA at 4°C and then transferred to PBS for further storage until processing. Optic nerves were dissected, embedded in 2% agar and then further embedded in paraffin wax [30].

Paraffin blocks were sectioned at 5  $\mu$ m thickness, deparaffinized, and rehydrated for IHC analysis. Sections were blocked with 5% normal goat serum and 1% bovine serum albumin in PBS for 30 minutes at room temperature to prevent non-specific binding. Slides were then incubated overnight at 4°C with primary antibody and then 1 hour at room temperature with the appropriate secondary antibody. Primary antibodies used were anti-total neurofilament (SMI-312, BioLegend, 1:300), anti-phosphorylated neurofilament (SMI-31, BioLegend, 1:300), and anti-myelin basic protein (MBP, Sigma, 1:300). Secondary antibodies were goat anti-mouse or goat anti-rabbit (Invitrogen, 1:240) with both conjugated to Alexa 488. Slides were mounted with Vectashield Mounting Medium for DAPI (Vector Laboratory, Inc., Burlingame, CA) and coverslipped. Images were acquired on a Nikon Eclipse 80i fluorescence microscope with MetaMorph software (Universal Imaging Corporation, Sunnyvale, CA) at 72 $\times$  and 84 $\times$  (1.2 and 1.4 magnification of 60 $\times$  objective) magnifications. Quantification was performed on entire optic nerve images which were the combination of four to six 72 $\times$  IHC images using ImageJ (<http://rsbweb.nih.gov/ij/plugins/volume-viewer.html>, NIH, US). Images were then undergone background subtraction, bilateral filter for edge preservation, watershed segmentation, threshold determination, and the analyze particles macro for SMI-312, SMI-31, and MBP area calculation and then normalized by entire area of optic nerve. Background subtraction, watershed segmentation, threshold determination, and analyze particles were used for DAPI counts.

### *Statistics*

For all the boxplots, whiskers extend to the minimum/maximum and the mean is marked as diamonds. Data were analyzed with a mixed effect linear model for Eye 1 vs. Eye 2 and baseline vs. Time 1 or Time 2. A first order auto-regressive covariance structure was used to account for

repeated-measures. The correlation of histology data and DBSI measurements at Time 2 were analyzed by Pearson's correlation.

## Results

### *Monocular visual acuity decrease at the onset of optic neuritis*

After immunization, daily visual acuity (VA) of EAE mice ( $n = 8$ ) was confirmed. When  $VA \leq 0.25$  c/d, defined as onset of optic neuritis (ON) [22], DBSI was performed and the eye was defined as Eye 1 at Time 1 ( $12.1 \pm 1.9$  days post-immunization, mean  $\pm$  SD,  $n = 8$ ). The other eye was defined as Eye 2. When the VA of Eye 2 decreased, DBSI was performed again at the same day ( $14.4 \pm 1.7$  days post-immunization, mean  $\pm$  SD,  $n = 8$ , one Eye 2 did not develop ON but still included in statistical analyses) defined as Time 2. The EAE mice in this cohort developed monocular lower VA at Time 1 and most Eye 2 showed lower VA 2 – 3 days later (Fig. 1).

### *DBSI reflected acute inflammation and axonal pathology specifically*

DTI- and DBSI-derived axial diffusivity ( $\lambda_{||}$ ) and radial diffusivity ( $\lambda_{\perp}$ ), and DBSI-restricted and DBSI non-restricted isotropic diffusion fraction maps from one representative Eye 1 were presented (Fig. 2). Decreased DTI  $\lambda_{||}$  but normal DBSI  $\lambda_{||}$  at Time 1 was seen with mild inflammatory cell infiltration and vasogenic edema, manifested as the increased DBSI restricted and non-restricted isotropic diffusion fractions. Both DTI and DBSI measurements showed decreased  $\lambda_{||}$  and increased  $\lambda_{\perp}$  at Time 2, suggesting axonal and myelin injury, respectively [16]. Comparing to DBSI measurements, exaggerated DTI  $\lambda_{||}$  and  $\lambda_{\perp}$  change at Time 2 were shown to parallel inflammatory cell infiltration and vasogenic edema as demonstrated by increased DBSI restricted and non-restricted isotropic diffusion fractions (Fig. 2). Group-averaged analyses for

Eye 1 and 2 from baseline, Time 1, and Time 2 were compared using box plots (Fig. 3). DTI-derived  $\lambda_{\parallel}$ ,  $\lambda_{\perp}$ , and FA reflected axonal damages over time (Fig. 3 A – C), revealing significantly decreased  $\lambda_{\parallel}$  at Time 1 and 2, significantly increased  $\lambda_{\perp}$  at Time 2, and significantly decreased FA in time 2. In contrast, the corresponding DBSI-derived pathological metrics exhibited no significant changes at Time 1 and a lesser, although significant, decrease in DBSI-  $\lambda_{\parallel}$  and FA at Time 2 (Fig. 3 D – F). Increased inflammatory cell infiltration (seen as increased DBSI restricted fraction, Fig. 3 G) and edema (as increased DBSI non-restricted fraction, Fig. 3 H) were clearly seen. The EAE mice in this cohort developed axonal injury (Fig. 3 D), mild demyelination (Fig. 3 E), and significantly increased cell infiltration (Fig. 3 G) and edema (Fig. 3 H) at acute ON.

#### *DBSI detected and quantified axonal loss in the presence of optic nerve swelling*

Onset of EAE ON was highly associated with inflammatory cell infiltration and edema, which led to optic nerve swelling in diffusion-weighted images (DWI, Fig. 4 A – C). Group-average of nerve volume showed significant swelling at Time 1 and 2 (Fig. 4 D). The corresponding DBSI-derived axon volume (nerve volume multiplying DBSI fiber fraction of corresponding ROI) demonstrated significant 18% and 17% axonal loss for Eye 1 and Eye 2 at Time 2, respectively (Fig. 4 E). DBSI fiber fraction correlated well with VA measurement from baseline to Time 2 (Fig. 4 F).

#### *Immunohistochemistry (IHC) of optic nerve*

Post-image SMI-312, SMI-31, MBP, and DAPI staining of optic nerves (Fig. 5) were used to assess axon and myelin integrity, and extent of cellularity. The EAE optic nerves showed significant axonal swelling in either severe or mild ON (yellow arrows, Fig. 5A) due to inflammation or axonal injury (red and white circles, Fig. 5 B and C). SMI-31, MBP, and SMI-

312 area fraction correlated well with DBSI  $\lambda_{\parallel}$ , DBSI  $\lambda_{\perp}$ , and DBSI fiber fraction, respectively (Fig. 6 A – C). DAPI counts correlated well with DBSI restricted fraction (Fig. 6 D). DBSI-derived axon volume, calculating by DWI-ROI-based nerve volume multiplying corresponding DBSI fiber fraction, correlated with SMI-312 area measured in mm<sup>2</sup> (without normalizing to optic nerve area, Fig. 6 E) at the onset of ON.

## Discussion

We examined optic nerve pathology in EAE mice at the onset of the ON when VA impairment was observed (Fig. 1). Optic neuritis in EAE mice, much like in MS, is heterogeneous in pathology with a mixture of axonal injury, demyelination, cellular inflammation and edema (Fig. 5) [22, 31–33]. We employed DBSI to monitor the evolving optic nerve pathology in EAE mice with ON by distinguishing and quantifying inflammation, demyelination, and axonal injury/loss simultaneously (Figs. 3, 4, and 6). DBSI revealed the presence of prominent inflammation-associated increase in cellularity and edema at the onset of ON (Fig. 3G – H), consistent with the postmortem IHC findings (Fig. 5, and 6). These pathological components, not only contributed to the impaired visual function but also confounded interpretation of DTI derived axonal injury and demyelination metrics (Fig. 3A – C).

Current MRI diagnostic approaches fail to accurately assess the progression of MS. Advanced MRI measures such as quantitative relaxation, diffusion, and magnetization transfer imaging provide more information than conventional MRI but unfortunately cannot distinguish between reversible and irreversible pathologies. The imaging markers sensitive and specific to axonal loss, which is irreversible, would provide the critical tools needed for assessing MS progression. The

advent of optical coherence tomography (OCT) has enabled the quantification of neuronal (ganglion cell layer/inner plexiform layer, GCL+IPL) and axonal (retinal nerve fiber layer, RNFL) loss in the visual system allowing the direct correlation of structure with function [34-36]. In MS patients with or without history of clinical optic neuritis, GCL+IPL and RNFL thinning have been reported [37, 38]. Interestingly, OCT-detected RNFL thinning has also been reported to correlate with brain atrophy [39-43]. The portions of the anterior visual pathway visualized using OCT have thus been considered to reflect central nervous system (CNS) integrity; OCT has increasingly been used as an outcome measure in MS [44-47].

Our results suggest that inflammation caused optic nerve swelling was prominent during acute ON (Fig. 4). Hence, OCT assessed RNFL thickness is likely confounded by the presence of acute inflammation [48]. The generality of OCT detected intraocular pathologies representing CNS pathologies outside of the visual system is also questionable since an association between brain parenchymal and intraocular atrophy does not prove that they are pathologically related. The posterior visual pathway (optic nerves/tracts/radiations) is not directly visualized by OCT due to the limited penetration of the technique. Thus, imaging biomarkers that can interrogate the entire CNS white matter, and distinguish and quantify different components of pathology without succumbing to their confounding interferences are greatly needed in MS.

We contend that DBSI would satisfy the unmet needs in MS and neurological disorders in general by providing specific pathological metrics reflecting axonal injury, demyelination, inflammation, and axonal loss. A longitudinal DBSI measurement could assess the effectiveness of anti-inflammatory therapies suppressing inflammation in real time. It would provide a means to

determine the effect of anti-inflammatory treatment on axonal preservation by longitudinally assessing axonal pathologies. Since axonal integrity plays a crucial role in neurological disability [49, 50], longitudinal measurements of DBSI-derived axonal volume could potentially quantify the rate of irreversible axonal loss and serve as a biomarker of MS progression preceding detectable clinical symptoms.

In summary, this study demonstrated the profile of VA and pathology for EAE mice at the onset of ON. The MR methodology, DBSI, we applied in this study enabled longitudinal assessment of the disease progression accurately. Therefore, DBSI holds potential as an outcome measurement for monitoring disease progression longitudinally corresponding to different severity of disability. DBSI meets the need for better understanding of disease progression and therapeutic effects for MS.

### **Acknowledgements**

This study was supported in part by the grants from National Institute of Health R01-NS047592 (S.-K.S.), P01-NS059560 (A.H.C.), National Multiple Sclerosis Society (NMSS) RG 4549A4/1 (S.-K.S.), and Department of Defense Idea Award W81XWH-12-1-0457 (S.-K.S.). AHC was supported in part by the Manny and Rosalyn Rosenthal-Dr. John L. Trotter MS Center Chair in Neuroimmunology of Barnes-Jewish Hospital Foundation.

### **Author Contributions**

CJPT, CWC, and THL conducted experiments, analyzed data, and jointly wrote the manuscript. YW and PS helped design the data processing routine, and helped analyzing DBSI data. MW helped with experiment design, and conducted the statistical analyses. RES helped with experiment design and pathology evaluation. AHC helped with experiment design and writing the manuscript. SKS designed experiments, the data processing routine, helped analyzing data and significantly contributed to the writing of the manuscript.

### **Conflicts of Interest**

The authors have no conflicts of interest to report.

## References

1. Bjartmar C, Kidd G, Mork S, Rudick R, Trapp BD: **Neurological disability correlates with spinal cord axonal loss and reduced N-acetyl aspartate in chronic multiple sclerosis patients.** *Annals of Neurology* 2000, **48**:893-901.
2. Kornek B, Lassmann H: **Axonal pathology in multiple sclerosis. A historical note.** *Brain Pathol* 1999, **9**:651-656.
3. Trapp BD, Peterson J, Ransohoff RM, Rudick R, Mork S, Bo L: **Axonal transection in the lesions of multiple sclerosis.** *N Engl J Med* 1998, **338**:278-285.
4. Trapp BD, Bo L, Mork S, Chang A: **Pathogenesis of tissue injury in MS lesions.** *J Neuroimmunol* 1999, **98**:49-56.
5. Lassmann H, van Horssen J, Mahad D: **Progressive multiple sclerosis: pathology and pathogenesis.** *Nat Rev Neurol* 2012, **8**:647-656.
6. Kamm CP, Uitdehaag BM, Polman CH: **Multiple sclerosis: current knowledge and future outlook.** *Eur Neurol* 2014, **72**:132-141.
7. Bitsch A, Schuchardt J, Bunkowski S, Kuhlmann T, Bruck W: **Acute axonal injury in multiple sclerosis. Correlation with demyelination and inflammation.** *Brain* 2000, **123 ( Pt 6)**:1174-1183.
8. Bjartmar C, Wujek JR, Trapp BD: **Axonal loss in the pathology of MS: consequences for understanding the progressive phase of the disease.** *J Neurol Sci* 2003, **206**:165-171.
9. Beck RW, Trobe JD, Moke PS, Gal RL, Xing D, Bhatti MT, Brodsky MC, Buckley EG, Chrousos GA, Corbett J, et al: **High- and low-risk profiles for the development of multiple sclerosis within 10 years after optic neuritis: experience of the optic neuritis treatment trial.** *Arch Ophthalmol* 2003, **121**:944-949.
10. Shams PN, Plant GT: **Optic neuritis: a review.** *Int MS J* 2009, **16**:82-89.
11. Torres-Torres R, Sanchez-Dalmau BF: **Treatment of acute optic neuritis and vision complaints in multiple sclerosis.** *Curr Treat Options Neurol* 2015, **17**:328.

12. Rueda-Lopes FC, Hygino da Cruz LC, Jr., Doring TM, Gasparetto EL: **Diffusion-weighted imaging and demyelinating diseases: new aspects of an old advanced sequence.** *AJR Am J Roentgenol* 2014, **202**:W34-42.
13. Narayana PA: **Magnetic resonance spectroscopy in the monitoring of multiple sclerosis.** *J Neuroimaging* 2005, **15**:46S-57S.
14. Mallik S, Samson RS, Wheeler-Kingshott CA, Miller DH: **Imaging outcomes for trials of remyelination in multiple sclerosis.** *J Neurol Neurosurg Psychiatry* 2014, **85**:1396-1404.
15. Song SK, Sun SW, Ramsbottom MJ, Chang C, Russell J, Cross AH: **Dysmyelination revealed through MRI as increased radial (but unchanged axial) diffusion of water.** *Neuroimage* 2002, **17**:1429-1436.
16. Song SK, Sun SW, Ju WK, Lin SJ, Cross AH, Neufeld AH: **Diffusion tensor imaging detects and differentiates axon and myelin degeneration in mouse optic nerve after retinal ischemia.** *Neuroimage* 2003, **20**:1714-1722.
17. Song SK, Yoshino J, Le TQ, Lin SJ, Sun SW, Cross AH, Armstrong RC: **Demyelination increases radial diffusivity in corpus callosum of mouse brain.** *Neuroimage* 2005, **26**:132-140.
18. Sun SW, Liang HF, Trinkaus K, Cross AH, Armstrong RC, Song SK: **Noninvasive detection of cuprizone induced axonal damage and demyelination in the mouse corpus callosum.** *Magn Reson Med* 2006, **55**:302-308.
19. Xie M, Tobin JE, Budde MD, Chen CI, Trinkaus K, Cross AH, McDaniel DP, Song SK, Armstrong RC: **Rostrocaudal analysis of corpus callosum demyelination and axon damage across disease stages refines diffusion tensor imaging correlations with pathological features.** *J Neuropathol Exp Neurol* 2010, **69**:704-716.
20. Wang Y, Wang Q, Haldar JP, Yeh FC, Xie M, Sun P, Tu TW, Trinkaus K, Klein RS, Cross AH, Song SK: **Quantification of increased cellularity during inflammatory demyelination.** *Brain* 2011, **134**:3590-3601.
21. Wang Y, Sun P, Wang Q, Trinkaus K, Schmidt RE, Naismith RT, Cross AH, Song SK: **Differentiation and quantification of inflammation, demyelination and axon injury or loss in multiple sclerosis.** *Brain* 2015, **138**:1223-1238.

22. Chiang CW, Wang Y, Sun P, Lin TH, Trinkaus K, Cross AH, Song SK: **Quantifying white matter tract diffusion parameters in the presence of increased extra-fiber cellularity and vasogenic edema.** *Neuroimage* 2014, **101**:310-319.

23. Lin TH, Kim JH, Perez-Torres C, Chiang CW, Trinkaus K, Cross AH, Song SK: **Axonal transport rate decreased at the onset of optic neuritis in EAE mice.** *Neuroimage* 2014, **100C**:244-253.

24. Tu TW, Budde MD, Xie M, Chen YJ, Wang Q, Quirk JD, Song SK: **Phase-aligned multiple spin-echo averaging: a simple way to improve signal-to-noise ratio of in vivo mouse spinal cord diffusion tensor image.** *Magn Reson Imaging* 2014, **32**:1335-1343.

25. Batchelor PG, Atkinson D, Hill DL, Calamante F, Connelly A: **Anisotropic noise propagation in diffusion tensor MRI sampling schemes.** *Magn Reson Med* 2003, **49**:1143-1151.

26. Wang X, Cusick MF, Wang Y, Sun P, Libbey JE, Trinkaus K, Fujinami RS, Song SK: **Diffusion basis spectrum imaging detects and distinguishes coexisting subclinical inflammation, demyelination and axonal injury in experimental autoimmune encephalomyelitis mice.** *Nmr in Biomedicine* 2014, **27**:843-852.

27. Wang X, Cusick MF, Wang Y, Sun P, Libbey JE, Trinkaus K, Fujinami RS, Song SK: **Diffusion basis spectrum imaging detects and distinguishes coexisting subclinical inflammation, demyelination and axonal injury in experimental autoimmune encephalomyelitis mice.** *NMR in Biomedicine* 2014.

28. Chiang CW, Wang Y, Sun P, Lin TH, Trinkaus K, Cross AH, Song SK: **Quantifying white matter tract diffusion parameters in the presence of increased extra-fiber cellularity and vasogenic edema.** *Neuroimage* 2014.

29. Wang Y, Wang Q, Haldar JP, Yeh FC, Xie M, Sun P, Trinkaus K, Klein RS, Cross A, Song S: **Quantification of increased cellularity during inflammatory demyelination.** *Brain* 2011, **134**:3587 - 3598.

30. Blewitt ES, Pogmore T, Talbot IC: **Double embedding in agar/paraffin wax as an aid to orientation of mucosal biopsies.** *J Clin Pathol* 1982, **35**:365.

31. Diem R, Demmer I, Boretius S, Merkler D, Schmelting B, Williams SK, Sattler MB, Bahr M, Michaelis T, Frahm J, et al: **Autoimmune optic neuritis in the common**

**marmoset monkey: comparison of visual evoked potentials with MRI and histopathology.** *Invest Ophthalmol Vis Sci* 2008, **49**:3707-3714.

32. Gold R, Linington C, Lassmann H: **Understanding pathogenesis and therapy of multiple sclerosis via animal models: 70 years of merits and culprits in experimental autoimmune encephalomyelitis research.** *Brain* 2006, **129**:1953-1971.
33. Sun SW, Liang HF, Schmidt RE, Cross AH, Song SK: **Selective vulnerability of cerebral white matter in a murine model of multiple sclerosis detected using diffusion tensor imaging.** *Neurobiol Dis* 2007, **28**:30-38.
34. Costello F, Coupland S, Hodge W, Lorello GR, Koroluk J, Pan YI, Freedman MS, Zackon DH, Kardon RH: **Quantifying axonal loss after optic neuritis with optical coherence tomography.** *Annals of Neurology* 2006, **59**:963-969.
35. Frohman EM, Fujimoto JG, Frohman TC, Calabresi PA, Cutter G, Balcer LJ: **Optical coherence tomography: a window into the mechanisms of multiple sclerosis.** *Nat Clin Pract Neurol* 2008, **4**:664-675.
36. Leung CK: **Diagnosing glaucoma progression with optical coherence tomography.** *Curr Opin Ophthalmol* 2014, **25**:104-111.
37. Walter SD, Ishikawa H, Galetta KM, Sakai RE, Feller DJ, Henderson SB, Wilson JA, Maguire MG, Galetta SL, Frohman E, et al: **Ganglion cell loss in relation to visual disability in multiple sclerosis.** *Ophthalmology* 2012, **119**:1250-1257.
38. Burkholder BM, Osborne B, Loguidice MJ, Bisker E, Frohman TC, Conger A, Ratchford JN, Warner C, Markowitz CE, Jacobs DA, et al: **Macular volume determined by optical coherence tomography as a measure of neuronal loss in multiple sclerosis.** *Arch Neurol* 2009, **66**:1366-1372.
39. Dorr J, Wernecke KD, Bock M, Gaede G, Wuerfel JT, Pfueller CF, Bellmann-Strobl J, Freing A, Brandt AU, Friedemann P: **Association of retinal and macular damage with brain atrophy in multiple sclerosis.** *PLoS One* 2011, **6**:e18132.
40. Gordon-Lipkin E, Chodkowski B, Reich DS, Smith SA, Pulicken M, Balcer LJ, Frohman EM, Cutter G, Calabresi PA: **Retinal nerve fiber layer is associated with brain atrophy in multiple sclerosis.** *Neurology* 2007, **69**:1603-1609.

41. Grazioli E, Zivadinov R, Weinstock-Guttman B, Lincoff N, Baier M, Wong JR, Hussein S, Cox JL, Hojnacki D, Ramanathan M: **Retinal nerve fiber layer thickness is associated with brain MRI outcomes in multiple sclerosis.** *J Neurol Sci* 2008, **268**:12-17.
42. Sepulcre J, Murie-Fernandez M, Salinas-Alaman A, Garcia-Layana A, Bejarano B, Villoslada P: **Diagnostic accuracy of retinal abnormalities in predicting disease activity in MS.** *Neurology* 2007, **68**:1488-1494.
43. Siger M, Dziegielewski K, Jasek L, Bieniek M, Nicpan A, Nawrocki J, Selmaj K: **Optical coherence tomography in multiple sclerosis: thickness of the retinal nerve fiber layer as a potential measure of axonal loss and brain atrophy.** *J Neurol* 2008, **255**:1555-1560.
44. Saidha S, Sotirchos ES, Oh J, Syc SB, Seigo MA, Shiee N, Eckstein C, Durbin MK, Oakley JD, Meyer SA, et al: **Relationships between retinal axonal and neuronal measures and global central nervous system pathology in multiple sclerosis.** *JAMA Neurol* 2013, **70**:34-43.
45. Calabresi PA, Balcer LJ, Frohman EM: **Retinal pathology in multiple sclerosis: insight into the mechanisms of neuronal pathology.** *Brain* 2010, **133**:1575-1577.
46. Balcer LJ: **Clinical trials to clinical use: using vision as a model for multiple sclerosis and beyond.** *J Neuroophthalmol* 2014, **34 Suppl**:S18-23.
47. Balcer LJ, Miller DH, Reingold SC, Cohen JA: **Vision and vision-related outcome measures in multiple sclerosis.** *Brain* 2015, **138**:11-27.
48. Syc SB, Saidha S, Newsome SD, Ratchford JN, Levy M, Ford E, Crainiceanu CM, Durbin MK, Oakley JD, Meyer SA, et al: **Optical coherence tomography segmentation reveals ganglion cell layer pathology after optic neuritis.** *Brain* 2012, **135**:521-533.
49. Kornek B, Storch MK, Weissert R, Wallstroem E, Stefferl A, Olsson T, Linington C, Schmidbauer M, Lassmann H: **Multiple sclerosis and chronic autoimmune encephalomyelitis: a comparative quantitative study of axonal injury in active, inactive, and remyelinated lesions.** *Am J Pathol* 2000, **157**:267-276.
50. Lassmann H: **Axonal injury in multiple sclerosis.** *J Neurol Neurosurg Psychiatry* 2003, **74**:695-697.

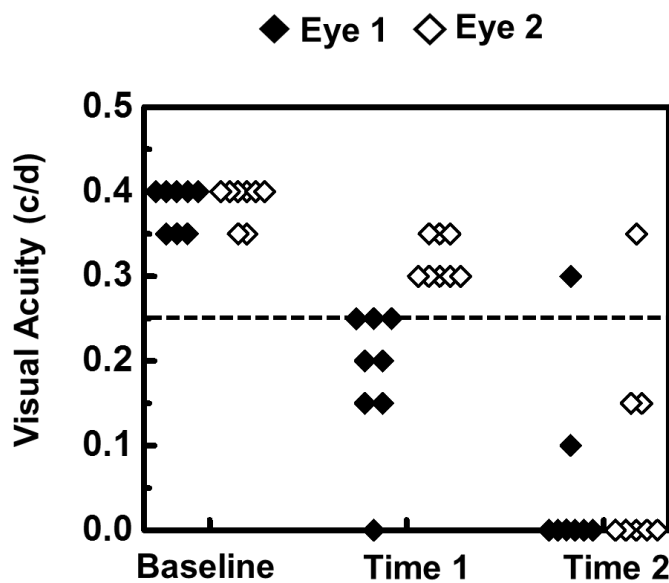


**Figure 1** Visual acuity (VA) of EAE mice ( $n = 8$ ) from baseline, pre-onset (Time 1 of Eye 2), onset (Time 1 of Eye 1 and Time 2 of Eye 2), and post-onset (Time 2 of Eye 1). Eye 1 = filled symbols; Eye 2 = open symbols. The dotted line indicates VA = 0.25 c/d, which was the threshold of defined onset of optic neuritis.

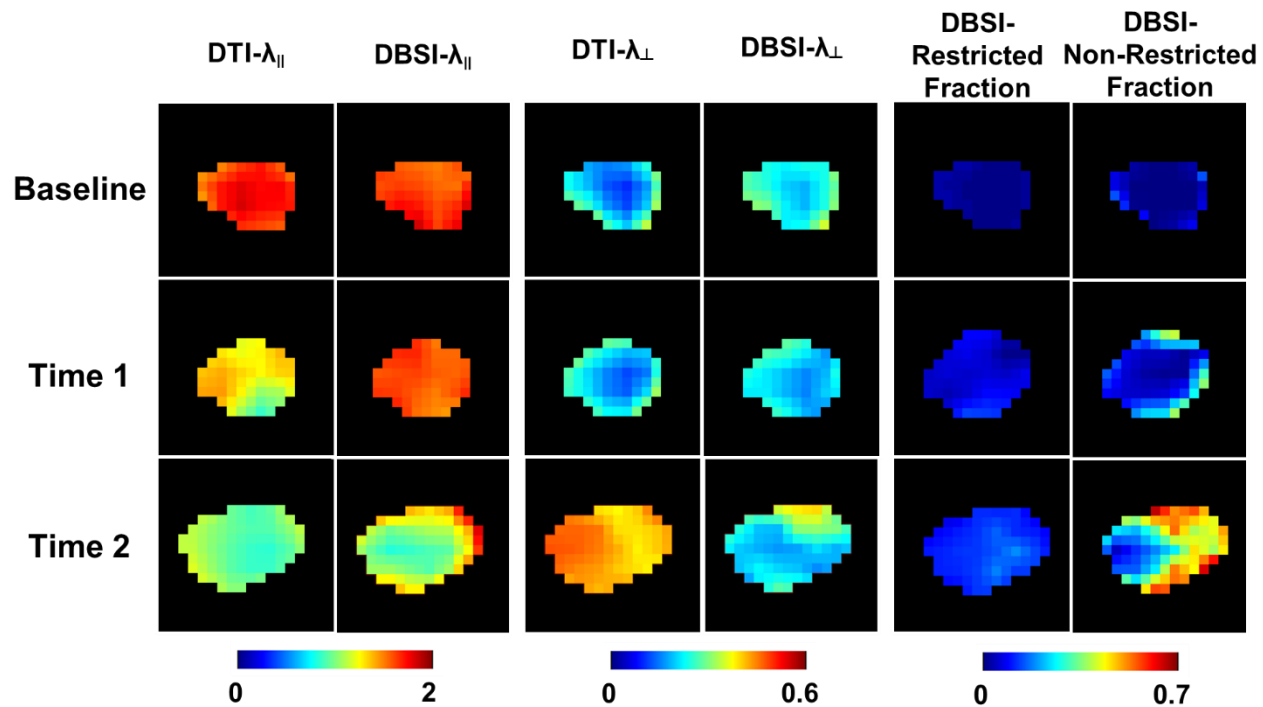


**Figure 2** DTI and DBSI derived parametric maps of one representative EAE optic nerve (Eye 1) from baseline (top row), Time 1 (middle row), and Time 2 (bottom row). Decreased axial diffusivity ( $\lambda_{\parallel}$ , columns 1 and 2) and increased radial diffusivity ( $\lambda_{\perp}$ , columns 3 and 4) in both DTI and DBSI measurements suggests axonal injury and demyelination at Time 2. DBSI further distinguished and quantified the extent of inflammatory cell infiltration (column 5) and vasogenic edema (column 6), which could not be detected by DTI confounding estimated  $\lambda_{\parallel}$  and  $\lambda_{\perp}$ .

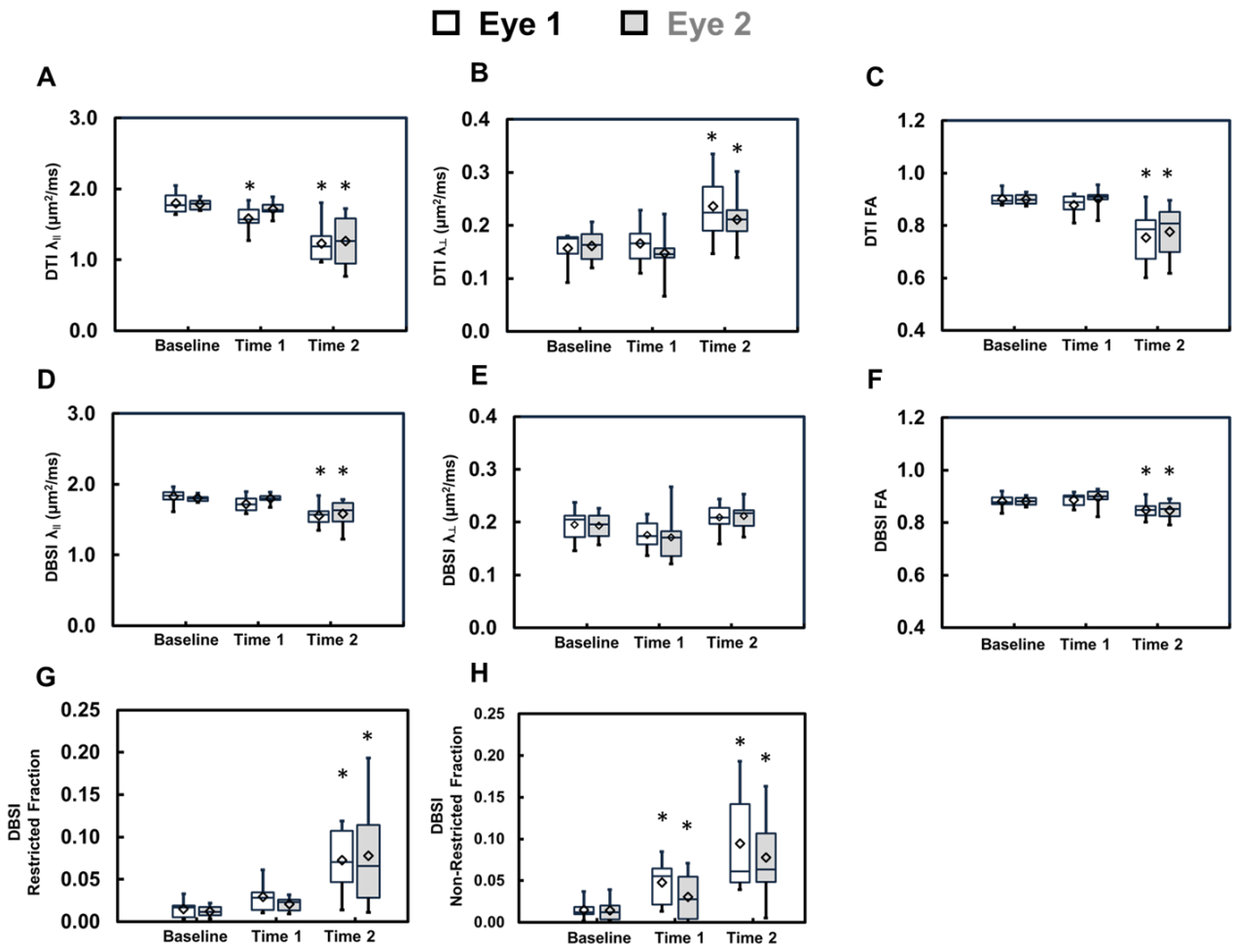


**Figure 3** Box plots summarize the group distribution of DTI-derived  $\lambda_{||}$ ,  $\lambda_{\perp}$  and FA (A – C) and DBSI-derived  $\lambda_{||}$ ,  $\lambda_{\perp}$ , FA, restricted, and non-restricted fraction (D – H) from baseline, Time 1, and Time 2 for Eye 1 (white box) and 2 (gray box), respectively. Both Eye 1 and 2 developed axonal injury at time 2 suggested by the significantly decreased DTI- and DBSI- $\lambda_{||}$  (A and D,  $p < 0.05$  for Eye 1 and 2). Both Eye 1 and 2 exhibited significantly increased DTI-  $\lambda_{\perp}$  ( $p < 0.05$  for Eye 1 and 2) but not in DBSI- $\lambda_{\perp}$  ( $p = 0.15$ ) at Time 2, reflecting the confounding effects of inflammatory cell infiltration and vasogenic edema (G and H,  $p < 0.05$  for Eye 1 and 2) on DTI-  $\lambda_{\perp}$ . The distribution of DBSI-FA (F, minimized confounding effects of inflammation) was much tighter than DTI-FA (C). DBSI results suggested that inflammatory cell infiltration and vasogenic edema was present at pre-onset (Eye 2, Time 1), onset (Eye 1, Time 1; Eye 2, Time 2), and post-onset (Eye 1, Time 2) of optic neuritis.

\* indicates  $p < 0.05$

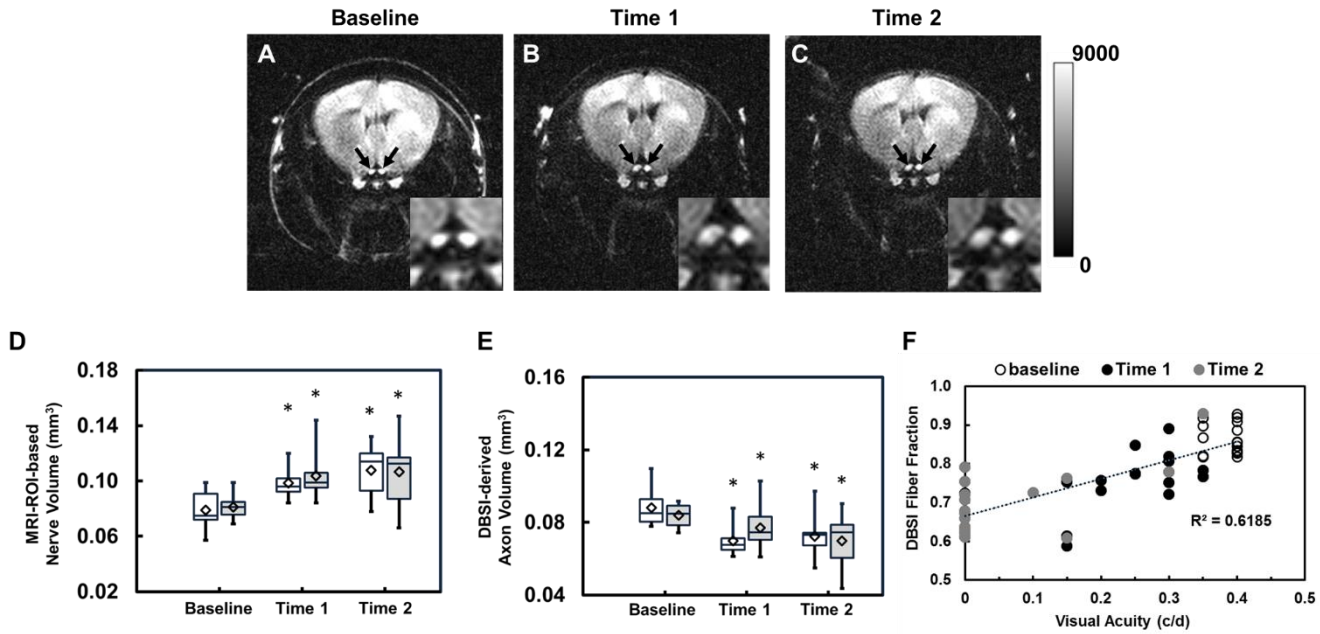


**Figure 4** Diffusion-weighted images (DWI) were acquired using the diffusion gradient applied perpendicular to the optic nerves (black arrows), at baseline (A, before EAE induction), Time 1 (B, onset of ON in the first eye), and Time 2 (C, onset of ON in the second eye) from an representative EAE mouse. Optic nerve swelling was seen at Time 1 and 2 caused by inflammation associated increase in cellularity and edema. Significantly increased optic nerve volume was seen after ON (D,  $p < 0.05$  for Eye 1 and 2). The corresponding DBSI-derived axon volume (optic nerve volume  $\times$  DBSI fiber fraction) suggested a significant axonal loss in optic nerves (E,  $p < 0.05$  for Eye 1 and 2). DBSI fiber fraction, reflecting effects of axonal loss and dilution effect of axonal density from inflammation, correlated well with visual acuity (F). \* indicates  $p < 0.05$ .

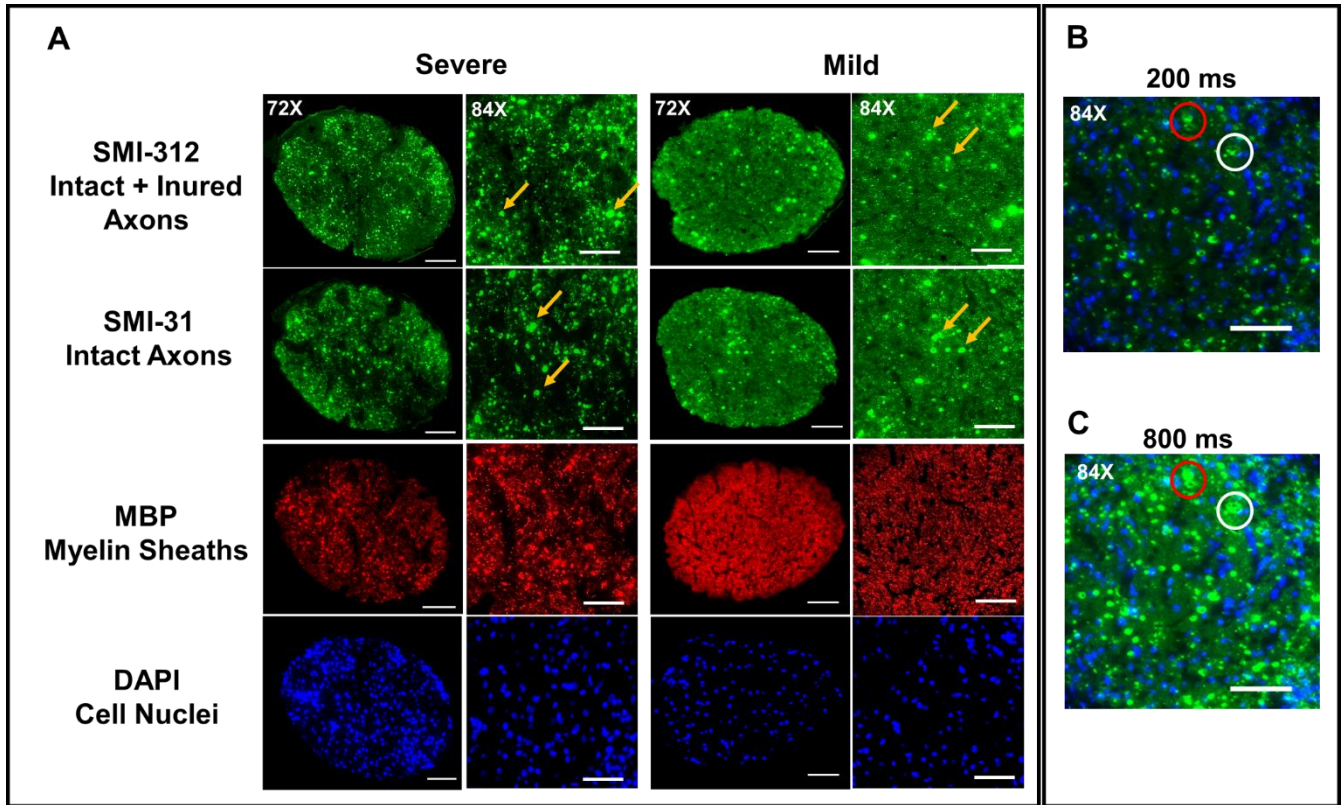


**Figure 5** Representative 72x immunohistochemical staining images of anti-total neurofilament (SMI-312, total axons), phosphorylated neurofilament (SMI-31, intact axon), myelin basic protein (MBP, myelin sheath), and 4', 6-dianidino-2-phenylindole (DAPI, nuclei) from severe (A, column 1) and mild (A, column 3) optic neuritis nerves demonstrate the different degrees of tissue damages. The corresponding 84x zoom-in images (covered ~50% of the optic nerve cross-section area) are displayed alongside 72x images (A, column 2 and 4, respectively). Swollen axons, some aggregated to form enlarged staining regions (A, yellow arrows), were seen in SMI-312 and SMI-31 staining images. Axonal loss and injury (reduced SMI-312 and SMI-31 positive staining), demyelination (decreased MBP positive staining), and cell infiltration (increased density of DAPI staining) were present in optic neuritis nerves. The zoom-in 84x DAPI and SMI-31 double-staining images from one EAE optic nerve with 200 ms (B) and 800 ms (C) exposure time revealed the multiple-axon aggregation underlying the unusually large green spots seen in the SMI-312 and SMI-31 images (B and C, red and white circles).

Scale bar: 50 µm

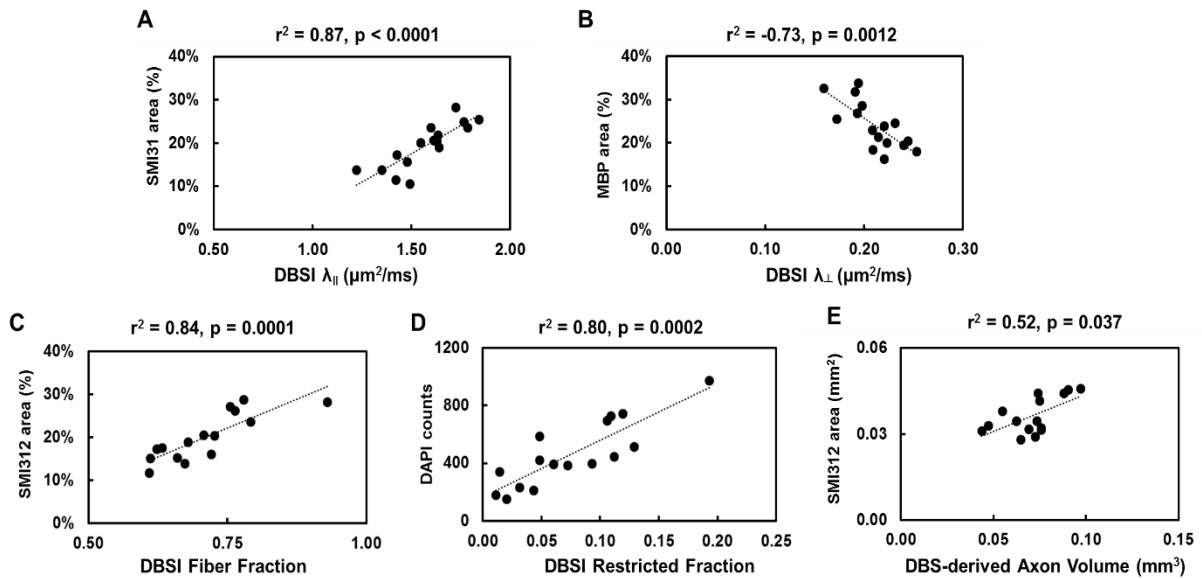


**Figure 6** DBSI derived  $\lambda_{\parallel}$ ,  $\lambda_{\perp}$ , fiber fraction, and restricted fraction correlated well with area ratios of SMI-31 (A), MBP (B), SMI-312 (C), and DAPI counts (D), respectively, suggesting that DBSI accurately reflected specific pathologies in the optic nerves of experimental autoimmune encephalomyelitis mice. The DBSI-derived axon volume correlated with SMI-312 area (in  $\text{mm}^2$ ). In contrast to SMI-312 area ratios, SMI-312 area reflects the extent of total axons without the dilution effect of inflammation.